SMGroup

SM Journal of Biomedical Engineering

Review Article

Analysis of the Cerebral Aneurysm Using Computational Fluid-Structure Interaction Model

Sana Sadeghi[1], Alireza Karimi[2], Kamran Hassani[1]*

[1]*Department of Biomechanics, Science and Research Branch, Islamic Azad University, Iran*
[2]*Tissue Engineering and Biological Systems Research Laboratory, Department of Biomechanics, School of Mechanical Engineering, Iran University of Science and Technology, Iran*

Article Information

Received date: Oct 18, 2015
Accepted date: Nov 30, 2015
Published date: Dec 02, 2015

***Corresponding author**

Kamran Hassani, Department of Biomechanics, College of Biomedical Engineering, Tehran Science and Research Branch, Islamic Azad University, Tehran, Iran, Email: k.hasani@srbiau.ac.ir

Keywords Cerebral Aneurysm; Fluid-Structure Interaction; Blood Flow; Dynamic of the Blood Flow; Hemodynamics

Abstract

The Fluid-Structure Interaction (FSI) computational method is in arising in the field of biomechanics. One of the most applicable problems in this area is the interaction of solid and fluid in the blood vessel. It may also have implication to understand the complexity of arterial diseases to figure out the interaction of fluid and arterial wall. So far many studies have been carried out to compute the stress and deformations of the blood in a cerebral aneurysm artery. Dynamic behavior of the blood in an artery would pave the way to understand the growth, rupture, and curing of the cerebral aneurysm. Therefore, in this study the dynamic behavior of the blood flow and its interaction with the basilar arterial wall was simulated using FSI approach. Thereafter, the von Mises stress, shear stress as well as deformations of both the arterial wall and blood were computed and compared to that of the healthy one. The mechanical behavior of the arterial wall was considered to be elastic, isotropic, homogenous, and incompressible, and the behavior of the blood flow was assumed to be laminar, Newtonian, and incompressible. The results of the present study may have implications for understanding the stresses and deformations of the blood flow in a healthy and basilar aneurysm artery.

Introduction

Cerebral Aneurysm (CA) is a cerebrovascular disorder in which weakness in the wall of a cerebral artery or vein causes a localized dilation or ballooning of the blood vessel [1]. Mostly, they produce at the bifurcation site of the large arteries and specifically in the Willis circle and those arteries which feed that. More than 85% of the aneurysms are placed in the anterior side of the blood circulatory system [2]. Furthermore, almost 15% of the aneurysms are placed in the posterior side of the Willis circle which ranked within the most vulnerable site of the basilar arteries [3,4]. The most common site for an arterial aneurysm is the abdominal aorta. A true aneurysm results from formation of a sac by the arterial wall with at least one unbroken layer [5]. As pointed out, aneurysm can be produced because of weakness of the arterial wall. As a result of that, the blood can pour out and fills the space around the artery and, finally, trigger hematoma [6]. Aneurysms can be distinguished according to their morphological characteristics. One of the most usual forms of the aneurysms is the one which named Congenital or Berry. This aneurysm seems like a seed which via a neck-like structure connects to the arteries [7]. The fusiform aneurysm is a spindle-shaped aneurysm. It is also a localized dilation of an artery in which the entire circumference of the vessel is distended. The result is an elongated, tubular, or spindle-like swelling. A giant intracranial aneurysm is defined as one larger than 2.5 cm in diameter. Treatment of large (2-2.5 cm) and giant aneurysms has traditionally been associated with a higher morbidity and mortality than smaller lesions [8,9]. Since the main reasons of initiation of the disease have not been well understood, there is still no comprehensive understanding for that. So far many researchers investigated the hemodynamic of the aneurysms, including blood pressure, velocity of the blood flow, shear stress of the arterial wall, in order to figure out the origination of the disease [10,11]. Eppinger was the first one who indicated that a weakness in the interior layer of the arterial wall leads to aneurysm [12]. Since the arterial wall is ranked within the soft biological tissues [13], it is intricate to have a precise mechanical model to define their behavior in the body. In addition, it is not possible to investigate the hemodynamics of the blood flow in an aneurysm artery in vivo [14]. Therefore, the application of modeling software, i.e., ABAQUS would pave the way to get the results as close as possible to the real condition of the human body [15]. However, it is obvious that the value of the results depend on the input data, such as mechanical behavior of the arterial wall as well as the blood flow [16,17].

Me, *et al.* [8] performed a numerical study to simulate a Three-Dimensional (3D) structure of a cerebral aneurysm using Magnetic Resonance Imaging (MRI). The structure of the aneurysm can be fall into different ones, including sphere, ellipsoid, and hemisphere. Parlea, *et al.* [18] employed a new pretty simple method to address the shape and size of the aneurysm in an artery wall.

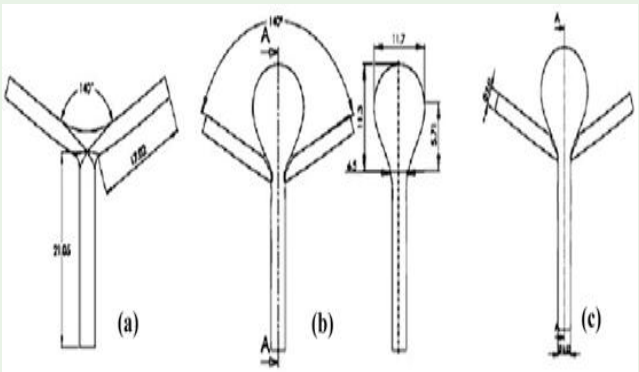

Figure 1: The structural model of (a) the healthy basilar artery and aneurysm one from the (b) side and (c) frontal view (all the dimensions are reported in mm).

In this study, a numerical modeling is carried out to simulate the 3D model of the aneurysm and compare it to that of a healthy one in a basilar artery. The structure of the aneurysm was adopted from the one in Figure 1. In order to do a more precise modeling, ABAQUS/CFD (Waltham, MA, the United States) was used to solve the incompressible flow and ABAQUS/Standard was used to solve the structural part of the model. To do this, at first the model was proposed to solve the hemodynamics of the flow using Computational Fluid Dynamics (CFD) of the blood flow, and then the interaction of the blood flow with that of the arterial wall was modeled using FSI approach. Thereafter, the shear stress, von Mises stress, displacement, and pressure of the diseased and healthy arteries are reported and compared.

Computational Model

Fluid and solid models

The blood flow in the model was considered to behave like a laminar, Newtonian, and incompressible fluid. The diameter for the inlet of the flow was 3.23 mm and the outlet was 2.41 mm, and the thickness of the arterial wall was also made as 300 μm. In addition, decreasing rate of the posterior artery of the brain was 0.75 times of the diameter of the basilar artery. The Reynolds number was also set to 422 [19]. Since the peak value of the Reynolds number at systolic side is 1620 and it is lower than the 2300, the inlet flow can be assumed to be laminar. The Arbitrary Lagrangian-Eulerian (ALE) method was employed to couple the solid (arterial wall) and fluid (blood) nodes together.

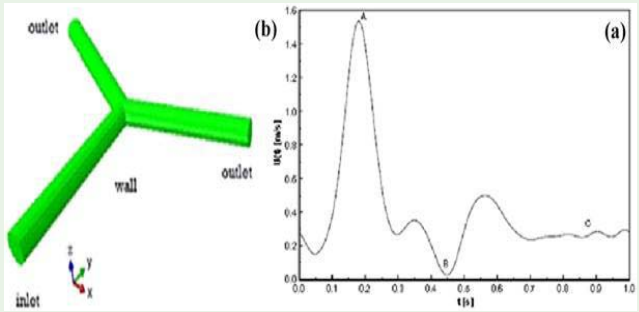

Figure 2: The (a) input velocity of the artery and (b) the boundary of the model for the simulation.

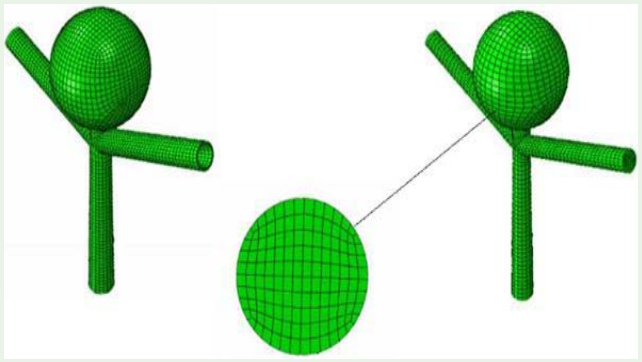

Figure 3: The meshed model of the aneurysm, including the CFD and Structure, by HEX elements.

$$\nabla.U = 0$$

$$\rho_f(\partial u)\partial t + ((u\text{-}u_g)).\nabla)u = \nabla p + \mu\nabla^2 u \quad (1)$$

where ρ_f is the fluid density, P is the pressure, u is the fluid velocity, and U_g is the vector of flow velocity. In the above equation, the term $(u\text{-}u_g)$ is the relative velocity of the flow in respect to the mean velocity [20]. In the current study, the blood was considered to be Newtonian with the density and dynamic viscosity of 1050 kg/m^3 and 0.00319 kg/m.s. Although the behavior of the blood flow is a non-Newtonian shear thinning, for the one which have a diameter larger than 0.5 mm the assumption of Newtonian flow is acceptable [21,22].

The momentum conservation equation for the mechanical behavior of the solid is presented in Equation 2.

$$\nabla.\sigma_s - \rho_s\dot{U}g \quad (2)$$

where ρ_s is the solid density, σ_s is the stress tensor, and $\dot{U}_g$ is the local acceleration of the solid. The mechanical behavior of the solid can be considered to be elastic [23-25] or hyperelastic [26,27], incompressible [28,29], and homogenous [30-32]. However, there are some other models which define the mechanical behavior of the arterial wall, including viscoelastic [33], hyperviscoleastic [34], etc. In the current study the mechanical behavior of the arterial wall was set to an isotropic elastic behavior with a Poisson's ratio of 0.45 and the density of 1050 kg/m^3 [35,36]. In addition, due to a small variation

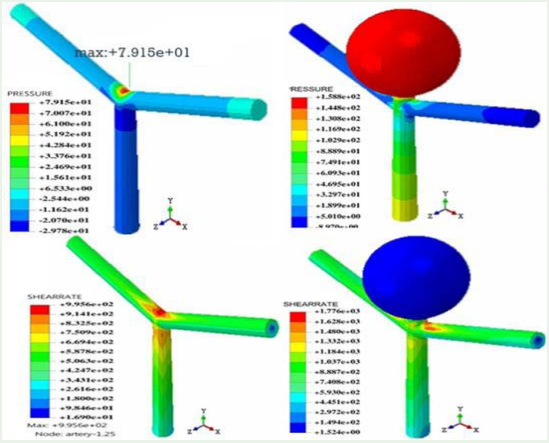

Figure 4: The pressure distribution and shear stress of the simulation model at the 0.2 sec.

Citation: Sadeghi S, Karimi A and Hassani K. Analysis of the Cerebral Aneurysm Using Computational Fluid-Structure Interaction Model. SM J Biomed Eng. 2015; 1(1): 1004.

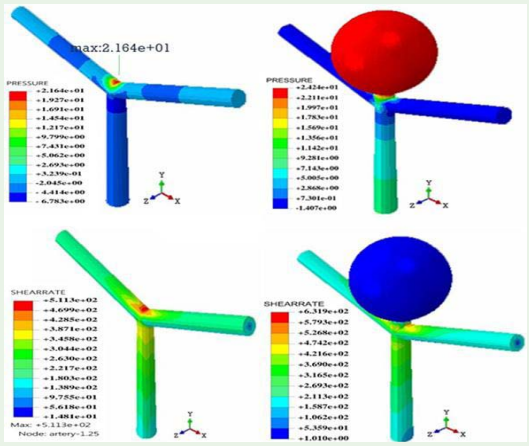

Figure 5: The pressure distribution and shear stress of the simulation model at the 0.4 sec.

is the blood flow, the blood was considered to be incompressible as well [37-39].

The geometry, boundary conditions, and methodology of the model

The structure of the model is indicated in Figure 1. The dimensions of the model are assigned to the model according to the Perlea, *et al.* [18]. The angle between the basilar artery and that of the posterior on in the brain was set to 140 which were calculated by Liou, *et al.* [40]. The length of the artery was defined as 6.1 and as 7.1 times larger than that of the diameter of the posterior and basilar artery of the brain [41]. The boundary of the fluid was divided into three regions, including inlet, outlet, and the transient (wall) sections as depicted in Figure 2. The boundary for the inlet of the flow was presumed to be pulsatile as plotted in Figure 2a and in the outlet section the pressure of zero with no slip boundary was defined as shown in the equations of 3 and 4 [42,43].

$$u|_{inlet} = u_t \tag{3}$$

$$\sigma_{nn}|_{outlet} = 0 \tag{4}$$

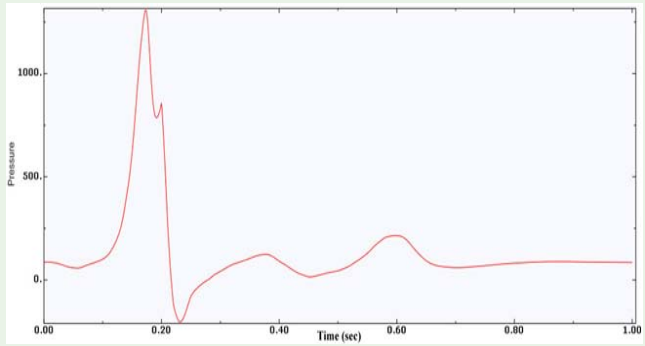

Figure 6: The curve of the pressure versus the simulation time for the basilar aneurysm artery.

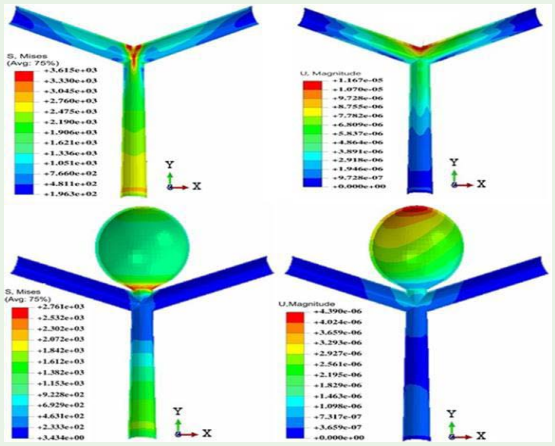

Figure 7: The distribution of the displacement as well as von Mises stress in the artery with and without aneurysm at the 0.2 sec.

The boundary for the solid was following the one in equation 5. In a way that, the displacement of the solid and fluid elements should agree with each other following the no slip boundary condition [44].

$$d_s = d_f \tag{5}$$

$$\acute{o}_s.\hat{n}_s = \acute{o}_f.\hat{n}_f \tag{6}$$

where σ, d, and $\hat{n}$ are the stress tensor, displacement, and normal vector in the boundary. The Terms s and f are also standing for solid and fluid, respectively. The velocity of the blood flow in the inlet of the main basilar artery was set to 39.7 m/s [41].

Meshing and mesh density analysis

In order to solve the numerical problem, including deformation and motion of the arterial wall, the suitable number of meshing is do required [45,46]. The model was meshed with Hex elements as illustrated in Figure 3. The blood flow was meshed with the FC3D8 elements. Five different meshing were compared from 3152 to 45652 and finally the mesh number of 11504 was selected since it showed suitable answer at a lower number of elements and simulation time.

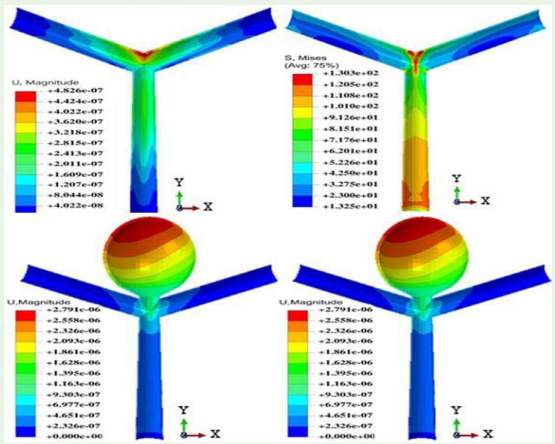

Figure 8: The distribution of the displacement as well as von Mises stress in the artery with and without aneurysm at the 0.4 sec.

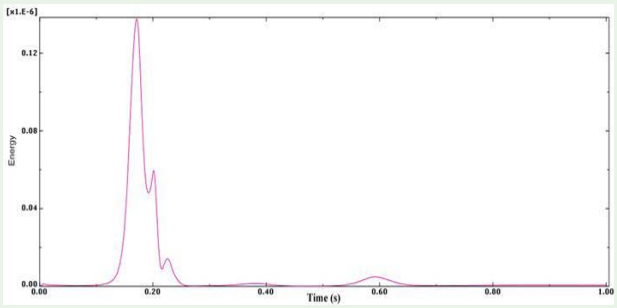

Figure 9: The curve of the energy for the aneurysm model.

Results

CFD modeling of the blood flow in the basilar artery

The blood flow was simulated with the boundary condition pointed out. Figure 4 shows the pressure distribution as well as the shear stress in the wall for the healthy and aneurysm basilar arterial walls. Degeneration of the weakness of the arterial wall is believed to be responsible of the hemodynamic stress in the bifurcation of the aneurysm wall [47]. In this figure, the pressure at the bifurcation point of the basilar artery at the simulation time of 0.2 sec which might be the reason of aneurysm is presented. In addition, the same pattern at the time of 0.4 sec is shown in Figure 5. The pressure curve versus the simulation time for the aneurysm basilar artery is provided in Figure 6. It is observed that the highest pressure is happened at the time of 0.2 sec when the shear stress reaches to its highest value.

Hemodynamics of the blood in the basilar aneurysm artery

The displacement and the von Mises stress of the arterial wall at the time of 0.2 and 0.4 sec are exhibited in Figures 7 and 8, respectively. The maximum amount of stress was occurred at the simulation time of 0.2 sec around the neck of aneurysm which may lead to rupture in the aneurysm wall. The results also showed that the displacement on the aneurysm wall is increasing from the neck of the aneurysm until the dome of that. Moreover, the displacement in the basilar artery as well as the posterior cerebral artery was almost zero. Finally, the distribution of energy in the aneurysm model is presented in Figure 9, which shows its highest value at the time of 0.2 sec.

Conclusions

In this study, the interaction of the blood flow and the aneurysm artery was simulated using a pulsatile computational FSI approach. Finally, the contours of stresses and strains were evaluated and compared for both the healthy and aneurysm basilar artery. The results of the present study may have implications for understanding the stresses and deformations of the blood flow in a healthy and basilar aneurysm artery.

References

1. Lasheras JC. The biomechanics of arterial aneurysms. Annu Rev Fluid Mech. 2007; 39: 293-319.
2. Karimi A, Navidbakhsh M, Alizadeh M, Shojaei A. A comparative study on the mechanical properties of the umbilical vein and umbilical artery under uniaxial loading. Artery Res. 2014; 8: 51-56.
3. Sweeting M, Ulug P, Powell J, Desgranges P, Balm R, Trialists RA. Ruptured Aneurysm Trials: The Importance of Longer-term Outcomes and Meta-analysis for 1-year Mortality. European J Vasc Endovasc Surg. 2015; 50: 297-302.
4. Abdi M, Karimi A, Navidbakhsh M, Pirzad Jahromi G, Hassani K. A lumped parameter mathematical model to analyze the effects of tachycardia and bradycardia on the cardiovascular system. Int J Numer Model: Electronic Networks, Devices Fields. 2015; 28: 346-357.
5. Alagheband M, Rahmani S, Alizadeh M, Karimi A, Navidbakhsh M. Hemodynamic investigation of intraluminal thrombus effect on the wall stress in a stented three-layered aortic aneurysm model under pulsatile flow. Artery Res. 2015; 10: 11-19.
6. Redcay E, Carlson TA. Rapid neural discrimination of communicative gestures. Social Cognitive Affective Neuroscience. 2015; 10: 545-551.
7. Barati E, Halabian M, Karimi A, Navidbakhsh M. Numerical evaluation of stenosis location effects on hemodynamics and shear stress through curved artery. J Biomater Tissue Eng. 2014; 4: 358-366.
8. Damiano RJ, Ma D, Xiang J, Siddiqui AH, Snyder KV, Meng H. Finite element modeling of endovascular coiling and flow diversion enables hemodynamic prediction of complex treatment strategies for intracranial aneurysm. J Biomech. 2015; 48: 3332-3340.
9. Abdi M, Karimi A. A computational electrical analogy model to evaluate the effect of internal carotid artery stenosis on circle of willis efferent arteries pressure. J Biomater Tissue Eng. 2014; 4: 749-754.
10. Sforza DM, Putman CM, Cebral JR. Hemodynamics of cerebral aneurysms. Annual Rev Fluid Mech. 2009; 41: 91-107.
11. Jeong W, Rhee K. Hemodynamics of cerebral aneurysms: computational analyses of aneurysm progress and treatment. Computational Mathematical Methods Medicine. 2012; 2012: 782801.
12. Atkinson JL, Sundt Jr TM, Houser OW, Whisnant JP. Angiographic frequency of anterior circulation intracranial aneurysms. J Neurosurgery. 1989; 70: 551-555.
13. Abdi M, Karimi A, Navidbakhsh M, Rahmati M, Hassani K. Modeling of coronary artery balloon-angioplasty using equivalent electrical circuit. Biomedical Engineering: Applications, Basis and Communications. 2014; 26: 1450039.
14. Halabian M, Karimi A, Beigzadeh B, Navidbakhsh M. A numerical study on the hemodynamic and shear stress of double aneurysm through S-shaped vessel. Biomedical Engineering: Applications, Basis and Communications. 2015; 27: 1550033.
15. Karimi A, Navidbakhsh M, Faghihi S, Shojaei A, Hassani K. A finite element investigation on plaque vulnerability in realistic healthy and atherosclerotic human coronary arteries. Proc IMech Part H. 2013; 227: 148-161.
16. Karimi A, Navidbakhsh M, Rezaee T, Hassani K. Measurement of the circumferential mechanical properties of the umbilical vein: experimental and numerical analyses. Computer Methods Biomech Biomed Eng. 2015; 18: 1418-1426.
17. Karimi A, Navidbakhsh M, Shojaei A, Hassani K, Faghihi S. Study of plaque vulnerability in coronary artery using Mooney–Rivlin model: a combination of finite element and experimental method. Biomedical Engineering: Applications, Basis and Communications. 2014; 26: 1450013.
18. Parlea L, Fahrig R, Holdsworth DW, Lownie SP. An analysis of the geometry of saccular intracranial aneurysms. Am J Neuroradiology. 1999; 20: 1079-1089.
19. Rahmani S, Alagheband M, Karimi A, Alizadeh M, Navidbakhsh M. Wall stress in media layer of stented three-layered aortic aneurysm at different intraluminal thrombus locations with pulsatile heart cycle. J Med Eng Tech. 2015; 39: 239-245.
20. Karimi A, Navidbakhsh M, Kudo S. A comparative study on the mechanical properties of the healthy and varicose human saphenous vein under uniaxial loading. J Med Eng Tech 2015; 39: 490-497.

21. Karimi A, Razaghi R, Shojaei A, Navidbakhsh M. An experimental-nonlinear finite element study of a balloon expandable stent inside a realistic stenotic human coronary artery to investigate plaque and arterial wall injury. Biomed Tech (Berl). 2015; 60: 593-602.

22. Karimi A, Navidbakhsh M, Yamada H, Razaghi R. A nonlinear finite element simulation of balloon expandable stent for assessment of plaque vulnerability inside a stenotic artery. Med Biol Eng Comput. 2014; 52: 589-599.

23. Karimi A, Navidbakhsh M, Alizadeh M, Razaghi R. A comparative study on the elastic modulus of polyvinyl alcohol sponge using different stress-strain definitions. Biomed Tech (Berl). 2014; 59: 439-446.

24. Karimi A, Navidbakhsh M. Material properties in unconfined compression of gelatin hydrogel for skin tissue engineering applications. Biomed Tech (Berl). 2014; 59: 479-486.

25. Karimi A, Haghighatnama M, Shojaei A, Navidbakhsh M, Haghi AM, Sadati SJA. Measurement of the viscoelastic mechanical properties of the skin tissue under uniaxial loading. Proc IMech Part L. 2015.

26. Karimi A, Rahmati SM, Navidbakhsh M. Mechanical characterization of the rat and mice skin tissues using histostructural and uniaxial data. Bioengineered. 2015; 6:153-160.

27. Karimi A, Haghighatnama M, Navidbakhsh M, Haghi AM. Measurement of the axial and circumferential mechanical properties of rat skin tissue at different anatomical locations. Biomed Tech (Berl). 2015; 60:115-122.

28. Karimi A, Navidbakhsh M, Haghighatnama M, Haghi AM. Determination of the axial and circumferential mechanical properties of the skin tissue using experimental testing and constitutive modeling. Computer Methods Biomechanics Biomedical Engineering. 2015; 18: 1768-1774.

29. Razaghi R, Karimi A, Rahmani S, Navidbakhsh M. A computational fluid–structure interaction model of the blood flow in the healthy and varicose saphenous vein. Vascular. 2015:1708538115594095.

30. Karimi A, Navidbakhsh M, Yousefi H. Mechanical properties of polyvinyl alcohol sponge under different strain rates. Int J Mater Res. 2014; 105: 404-408.

31. Karimi A, Navidbakhsh M. Measurement of the nonlinear mechanical properties of a poly (vinyl alcohol) sponge under longitudinal and circumferential loading. J Appl Polym Sci. 2014; 131.

32. Karimi A, Navidbakhsh M. An experimental study on the mechanical properties of rat brain tissue using different stress–strain definitions. J Mater Sci: Mater Med. 2014; 25: 1623-1630.

33. Karimi A, Navidbakhsh M, Beigzadeh B. A visco-hyperelastic constitutive approach for modeling polyvinyl alcohol sponge. Tissue Cell. 2014; 46: 97-102.

34. Karimi A, Navidbakhsh M. Mechanical properties of PVA material for tissue engineering applications. Mater Tech Adv Perform Mater. 2014; 29: 90-100.

35. Karimi A, Navidbakhsh M, Shojaei A, Faghihi S. Measurement of the uniaxial mechanical properties of healthy and atherosclerotic human coronary arteries. Mater Sci Eng C Mater Biol Appl. 2013; 33: 2550-2554.

36. Jarrahi A, Karimi A, Navidbakhsh M, Ahmadi H. Experimental/numerical study to assess mechanical properties of healthy and Marfan syndrome ascending thoracic aorta under axial and circumferential loading. Mater Tech Adv Perform Mater. 2015.

37. Khoushkar A, Marefat M, Mokhtari DM. Suggesting A new model for arterial pressure gradient by measuring the centerline veloity of artery using ultrasonic method. 2005; 7: 41-48.

38. Karimi A, Navidbakhsh M. A comparative study on the uniaxial mechanical properties of the umbilical vein and umbilical artery using different stress–strain definitions. Australas Phys Eng Sci Med. 2014; 37: 645-654.

39. Karimi A, Navidbakhsh M, Shojaei A. A combination of histological analyses and uniaxial tensile tests to determine the material coefficients of the healthy and atherosclerotic human coronary arteries. Tissue Cell. 2015; 47: 152-158.

40. Liou T-M, Liou S-N. A review on in vitro studies of hemodynamic characteristics in terminal and lateral aneurysm models. Proceedings of the National Science Council, Republic of China Part B, Life Sci. 1999; 23: 133-148.

41. Valencia A, Solis F. Blood flow dynamics and arterial wall interaction in a saccular aneurysm model of the basilar artery. Computers Structures. 2006; 84: 1326-1337.

42. Karimi A, Navidbakhsh M, Razaghi R, Haghpanahi M. A computational fluid-structure interaction model for plaque vulnerability assessment in atherosclerotic human coronary arteries. J Appl Phys. 2014; 115: 144702.

43. Karimi A, Navidbakhsh M, Razaghi R. A finite element study of balloon expandable stent for plaque and arterial wall vulnerability assessment. J Appl Phys. 2014; 116: 044701.

44. Karimi A, Navidbakhsh M, Razaghi R. Plaque and arterial vulnerability investigation in a three-layer atherosclerotic human coronary artery using computational fluid-structure interaction method. J Appl Phys. 2014; 116: 064701.

45. Rezaei F, Hassani K, Solhjoei N, Karimi A. Carbon/PEEK composite materials as an alternative for stainless steel/titanium hip prosthesis: a finite element study. Australas Phys Eng Sci Med. 2015.

46. Karimi A, Razaghi R, Kudo S, Navidbakhsh M. Dynamic Finite Element Simulation of the Human Head Under Impact Loading to Compare the Application of Polyvinyl Alcohol Sponge and Expanded Polystyrene Foam as Helmet Materials. J Adv Phys. 2016; 5: 159-165.

47. Guglielmi G, Viñuela F, Duckwiler G, Dion J, Lylyk P, Berenstein A, et al. Endovascular treatment of posterior circulation aneurysms by electrothrombosis using electrically detachable coils. J Neurosurgery. 1992; 77: 515-524.